# Development of a new model of reconstituted mouse epidermis and characterization of its response to proinflammatory cytokines

Mathilde Pohin, Carolina Veaute, Julien Garnier, Christine Barrault, Laure Cronier, Vincent Huguier, Laure Favot, Jiad Mcheik, François-Xavier Bernard, Jean-Claude Lecron, et al.

# Development of a new model of reconstituted mouse epidermis and characterization of its response to proinflammatory cytokines

Mathilde Pohin[1], Carolina Veaute[2], Julien Garnier[3], Christine Barrault[3], Laurent Cronier[4], Vincent Huguier[1,5], Laure Favot[1], Jiad Mcheik[1,5], François-Xavier Bernard[1,3], Jean-Claude Lecron[1,5], Franck Morel[1] and Jean-François Jégou[1*]

[1]Laboratoire Inflammation, Tissus Epithéliaux et Cytokines (LITEC), EA 4331, Université de Poitiers, France

[2]Laboratorio de Inmunología Básica, Facultad de Bioquímica y Ciencias Biológicas, Universidad Nacional del Litoral, Santa Fe, Argentina

[3]Bioalternatives, Gençay, France

[4]STIM, CNRS ERL 7368, Université de Poitiers, Poitiers, France

[5]CHU de Poitiers, France

Running title: New model of reconstituted mouse epidermis.

Keywords: three-dimensional culture, keratinocyte, reconstituted epidermis, skin inflammation, cytokine.

*Correspondence to: Dr. Jean-François Jégou, Laboratoire Inflammation, Tissus Epithéliaux et Cytokines, UPRES EA 4331, Pôle Biologie Santé, Université de Poitiers, 1 Rue Georges Bonnet, TSA 51106, 86073 POITIERS Cedex 9, France; Phone: +33.5.49.45.36.45. ; Fax: +33.5.49.45.49.86; E-mail address: jean-francois.jegou@univ-poitiers.fr

## Abstract

The development of three-dimensional models of reconstituted mouse epidermis (RME) has been hampered by the difficulty to maintain murine primary keratinocyte cultures and to achieve a complete epidermal stratification. In this study, we propose a new protocol for the rapid and convenient generation of RME, which reproduces accurately the architecture of a normal mouse epidermis. During RME morphogenesis, the expression of differentiation markers such as keratins, loricrin, filaggrin, E-cadherin and connexins was followed, showing that RME structure at day 5 was similar to those of a normal mouse epidermis, with the acquisition of the natural barrier function. We also demonstrated that RME responded to skin-relevant proinflammatory cytokines by increasing the expression of antimicrobial peptides and chemokines, and inhibiting epidermal differentiation markers, as in the human system. This new model of RME is therefore suitable to further investigate mouse epidermis physiology and opens new perspectives to generate reconstituted epidermis from transgenic mice.

## 1. Introduction

In the field of immunodermatology research, standard monolayer cell cultures of human keratinocytes are commonly used for *in vitro* studies, although they do not completely recapitulate the physiological skin architecture and the features of the different states of cell differentiation. The stratification of keratinocytes is essential to study the physiological response of the epidermis since keratinocytes from the basal layer are widely different from corneocytes in morphology but also in metabolism and response to environmental factors. Regarding those limits, three-dimensional models of reconstituted human epidermis (RHE) have been therefore developed and proved to be more suitable to test cosmetics products, for drug development or cutaneous disease modelling. Mouse is also commonly used to investigate human diseases *in vivo*, offering a large possibility of spontaneous, genetically engineered or inducible murine models of skin pathologies. By contrast to human primary keratinocytes, murine keratinocytes have always been difficult to isolate and to maintain in culture. Likewise, the development of reconstituted murine epidermis (RME) seems to be more problematic to achieve a complete stratification than RHE.

Over the last three decades, the development of RHE consisted in determining the optimal culture conditions to reach a rapid and complete epidermal differentiation. The first attempts described the need for cultivating keratinocytes on irradiated fibroblastic feeder cells, in culture medium supplemented with epidermal growth factor and hydrocortisone, but resulted in an incomplete stratification of keratinocyte colonies (Rheinwald and Green, 1975). The capacity of keratinocytes cultivated in monolayer to differentiate into three-dimensional epidermis was further shown to require their transition to an air/liquid interface (Prunieras, *et al.*, 1983, Rosdy and Clauss, 1990). Then, the modulation of calcium concentrations in culture medium has been identified as key element in regulating the proliferation/differentiation

balance (Hennings, *et al.*, 1980). Calcium has also been reported to play a role in adherent junctions through the assembly of the E-cadherins (Tu and Bikle, 2013, Tu, *et al.*, 2008). Finally, the substitution of the classic fetal bovine serum in culture media by specific growth factors such as keratinocyte growth factor (KGF), bovine pituitary extract, Insulin Growth Factor and L-acid ascorbic allowed to get rid of fibroblastic feeders and was shown to induce a better epidermal stratification with the restoration of the natural barrier function (Bertolero, *et al.*, 1984, Borowiec, *et al.*, 2013, Frankart, *et al.*, 2012, Ponec, *et al.*, 1997, Rosdy and Clauss, 1990).

Attempting to develop RME, some authors used human de-epidermized dermis (Carroll and Moles, 2000) or employed mouse dermal fibroblasts as feeders for keratinocyte attachment and growth (Ikuta, *et al.*, 2006, Rosenberger, *et al.*, 2014). This fibroblastic support was demonstrated to favor the establishment of the epidermis and to improve long term skin equivalents (Boehnke, *et al.*, 2007). With technical progress in the characterization of stem cells, some studies described long-term protocol to generate mouse epidermal stem and precursor cell lines (Segrelles, *et al.*, 2011, Vollmers, *et al.*, 2012). After several passages, epidermal progenitor cell lines were successfully obtained and used to generate mouse reconstructed epidermis. In these models, the epidermal differentiation remained limited as indicated by the discontinued expression of some differentiation markers such as keratin (K) 10, involucrin or loricrin by suprabasal keratinocytes.

The differentiation of keratinocytes is a complex molecular process which leads to the establishment of a protective barrier. It results in a spatiotemporal expression of epidermal differentiation markers. In the basal layer, K5/K14 are expressed by undifferentiated keratinocytes and K6/16 expressions are restricted to hyperproliferative or activated keratinocytes (Moll, *et al.*, 2008), while K1/K10 expressions are found in the differentiated keratinocytes of the suprabasal layers (Simpson, *et al.*, 2011). In the granular layer,

keratinocytes expressed progressively involucrin and loricrin which are involved in the formation of the mature cornified envelope. Granular keratinocytes are also characterized by the presence of keratohyalin granules in their cytoplasm, containing the pro-filaggrin. In the upper layers, filaggrin aggregates with the intermediate K1/K10 filaments to form mature corneocytes and contributes to the epidermal barrier function (Candi, *et al.*, 2005, Pendaries, *et al.*, 2014). In addition, GAP junctions were shown to be essential for the communication between keratinocytes throughout the epidermis. Among the connexins (Cx) found in the epidermis, Cx43 is highly expressed in the basal and spinous layers, whereas Cx26 expression is restricted to the granular layer (Kandyba, *et al.*, 2008, Scott, *et al.*, 2012).

In inflammatory conditions, this epidermal differentiation is altered and the protective barrier may be disrupted. RHE have been commonly used *in vitro* to study the effect of proinflammatory mediators which were reported to be overexpressed in different skin pathologies. We and others reported the activity of cytokines, such as IL17A, IL-1α, TNFα, IL-22 and Oncostatin M (OSM), alone or in synergy, on epidermal differentiation, recapitulating some features of psoriasis or atopic dermatitis (Boniface, *et al.*, 2005, Boniface, *et al.*, 2007, Guilloteau, *et al.*, 2010, Pohin, *et al.*, 2016, Rabeony, *et al.*, 2014, Rabeony, *et al.*, 2015, Wilson, *et al.*, 2007). OSM and IL-22 induced the expression of K6, classically associated with keratinocyte proliferation, and inhibited the expression of differentiation markers such as K10, filaggrin, involucrin and loricrin leading to epidermis hyperplasia (Rabeony, *et al.*, 2014). By contrast, IL-1α, IL-17A and TNF-α were found to be more important for innate immune activation, by inducing higher expressions of proinflammatory mediators by keratinocytes such as chemokines (CXCL-3), or the antimicrobial peptides β-defensin 3 (BD3) and S100A9 (Guilloteau, *et al.*, 2010).

Here, we described a fast and convenient method to generate RME using primary keratinocyte cultures from newborn mouse skin, without fibroblastic support, which reproduce accurately

the morphological features of a normal murine epidermis. In this study, we characterized the progressive morphogenesis of the epidermis and the expression profiles of proteins involved in differentiation, as well as the expression of proinflammatory cytokine receptors. Finally, we performed functional studies on RME, by analyzing their natural barrier function and their response to proinflammatory cytokines.

## 2. Materials and methods

### 2.1. Generation of Reconstituted Murine Epidermis

Normal Murine Epidermal Keratinocytes (NMEK) were isolated from pooled skins of C57BL/6J newborn mice and cultivated in CnT07 medium (CELLnTEC) as previously described (Pohin, *et al.*, 2016). After 5 days, when cells reached 80% of confluency, they were detached with Trypsin LE-express (Invitrogen) and centrifuged at 1500 rpm for 5 min, before resuspension at $1.125\times10^6$ cells/ml in CnT07 medium. Polycarbonate culture inserts (0.63 $cm^2$ of area containing 0.4 µm diameter pore size, Millipore) were seeded with 400 µl of cell suspension ($0.45\times10^6$ cells) and deposited in the bottom of six-well plates containing 3 ml of CnT07 medium with 1.5 mM of calcium. After 24 h of incubation at 37°C in a humidified atmosphere containing 5% $CO_2$, keratinocytes were exposed to the air/liquid interface by adding a sterile gaze under the insert in each well and replacing the CnT07 medium by 3 ml of differentiation medium composed of Epilife medium with HKGS supplements (Cascade biologics), 1.5 mM of calcium, 50 µg/ml of L-ascorbic acid (Sigma) and 3 ng/ml of murine recombinant KGF (R&D systems). This medium was renewed every 2 days until the use of RME.

### 2.2. Cytokines stimulation

Five days after the air/liquid interface exposure, RME were stimulated with the murine cytokines OSM, IL-22, IL-17A, IL-1α and TNF-α (10 ng/ml, R&D systems) or a mix of the five cytokines at 10 ng/ml or 1 ng/ml each, for 24 h before transcriptional analyses or for 72 h before histology, ELISA and permeability studies.

### 2.3. RNA and real-time quantitative RT-PCR

Total RNA was extracted from RME using Nucleospin RNA XS kit (Macherey-Nagel). RNA was reverse-transcribed with Superscript II Reverse Transcriptase (Invitrogen) and transcripts were amplified and quantified using the LightCycler-FastStart DNA Master Plus SYBR Green I kit on a LightCycler 480 instrument (Roche). Oligonucleotides were designed with Primer-Blast software, purchased from Eurogentec and listed in Supporting Information Table 1. Samples were normalized to the expression of the control housekeeping gene, *GAPDH*, or reported according to the ΔΔCT method as RNA fold change: $2^{\Delta\Delta CT} = 2^{\Delta CT \text{ sample} - \Delta CT \text{ reference}}$, as indicated in the figure legends.

### 2.4. Histology and immunohistofluorescence

For histological examination, RME were fixed in 4% formaldehyde before inclusion in paraffin and H&E coloration. For immunohistofluorescence, frozen sections (8 µm-thick) embedded in Cryomatrix compound (Shandon) were fixed either in cold acetone/methanol (20/80, v/v) for 10 min or in 4% paraformaldehyde/PBS solution (only for Cx26, Cx43 and E-Cadherin immunostainings). After blocking with 0.5 to 2% FBS or BSA solutions and permeabilization in 0,5% Triton X-100 diluted in PBS, samples were incubated with primary antibodies directed against the following mouse antigens: K6 (Thermo Scientific), K14, K10, filaggrin, loricrin (all from Covance), Cx26 (Invitrogen), Cx43 (BD Biosciences), E-cadherin (SC-7870, Santa-Cruz). RRX- or FITC- conjugated goat or donkey antibodies were used as secondary antibodies (Jackson Immunoresearch). Cell nuclei were stained with TOPRO-3 (Molecular Probes). Image acquisition was performed with an Olympus FV1000 confocal microscope using FluoView software (ImageUP platform, Université de Poitiers).

### 2.5. Lucifer Yellow permeability assay and ELISA

Lucifer Yellow (LY, 200 µl of 1 mM solution; Sigma) was deposited inside the insert on the surface of RME and incubated for 6 h at 37°C, 5% $CO_2$. Frozen sections were fixed in 4%

formaldehyde. Image acquisition was performed with an Olympus FV1000 confocal microscope using FluoView software (ImageUP platform, Université de Poitiers). To assess RME permeability, concentrations of LY that passed through RME were measured in culture medium using a Varioskan Flash at 550 nm emission (Thermo scientific). To investigate the role of connexins in the barrier function of RME, carbenoxolone (CBX , Sigma) was used to block gap junctions at a non-cytotoxic concentration of 60 µM.

ELISA for mouse S100A9 detection was provided with R&D Systems and carried out according to the manufacturer's instructions.

# 3. Results

## 3.1. Epidermal morphogenesis and localization of differentiation markers in RME mimic a normal epidermis

We have designed a new protocol for the rapid, convenient and reproducible generation of RME using keratinocytes isolated from newborn mouse skin, requiring no fibroblastic support or de-epidermised dermis, which allows studying exclusively the physiology of epidermis independently of dermis influence. Freshly isolated murine primary keratinocytes were directly seeded in polycarbonate membrane inserts to form the future RME as described in the experimental procedures (Figure 1A). The protocol to reach a complete epidermal stratification in the mouse system has been adapted from protocols previously described for human three-dimensional equivalents (Frankart, *et al.*, 2012, Guenou, *et al.*, 2009, Poumay and Coquette, 2007). This adaptation for RME consisted mainly in incubating firstly keratinocytes in a seeding medium composed of CnT07 medium, adapted for murine cell culture, with an increased calcium concentration (1.5 mM) to form a regular cell monolayer, then in incubating the cells, after their passage to the air-liquid interface, in a differentiation medium composed of complete Epilife medium supplemented with murine KGF, L-ascorbic acid and high calcium concentration. In order to monitor the epidermal morphogenesis of the RME, histological analyses and fluorescent immunostaining of several differentiation markers were performed at day 3, 5 and 8 after exposure to the air/liquid interface, and compared with normal epidermis (Figure 1B). Histological examination after H&E staining showed that RME exhibited a single layer of confluent keratinocytes at day 3, covered by a protective layer of acidophilic keratinocytes as previously described in human RHE (Frankart, *et al.*, 2012). At day 5, RME were ~ 20 µm thick and displayed a complete epidermis morphogenesis with the presence of the four expected layers. Notably, we could observe the

presence of keratohyalin granules in the granular layer and a thin corneous layer. After 8 days, histological analyses of RME showed a dense corneous layer, RME degenerating progressively in differentiated corneocytes. K6 expression is normally restricted to hyperproliferative cells of the basal layer in normal epidermis but it was expressed throughout the RME at day 3. This expression was maintained at day 5 and clearly lowered at day 8. As expected, K14 expression was restricted to the basal layer at all time points assessed, while K10, loricrin and filaggrin were weakly expressed by RME at day 3. At day 5, RME exhibited a strong K10 immunostaining throughout the suprabasal layer and both expressions of filaggrin and loricrin in the granular and the corneous layers, respectively, were similar to those observed in normal epidermis from adult mice. In conclusion, it appears that RME at day 5 reproduces accurately the morphology of a normal epidermis and the expression profile of epidermal markers.

### 3.2. RME form a cohesive tissue and an efficient barrier.

The appropriate cohesion of keratinocytes in a three-dimensional reconstituted epidermis is also dependent on the expression of proteins of adherent junctions and connexins (Cx) involved in GAP junctions. All over the epidermis, E-cadherin was expressed in the intercellular space of the RME from day 3 and was maintained up to day 8, like in a normal mouse epidermis (Figure 2A). Cx43 was found in the basal and spinous layers of a mature epidermis from day 3 to day 8, harboring the characteristic punctiform immunostaining observed in the normal epidermis (Figure 2A). RME highly expressed Cx26 at day 5 and 8, with a localization more restricted to the granular layer. Nonetheless, the expression seemed to be more sustained in the *in vitro* model compared to the normal epidermis (Figure 2A).

To confirm that RME acquired their natural barrier function, we have applied the hydrophilic fluorescent dye Lucifer Yellow (LY) on the top of each RME on day 0, 3, 5 and 8 for 6 h. The

analysis of concentrations of LY that diffused through the RME showed that the dye start to be retained at day 0 (~ 98% of retention), when keratinocytes form only a monolayer (Figure 2B). RME were effectively impermeable to LY from day 3 to day 8 (Figure 2B), LY being mainly retained in the cornified layer as observed by confocal microscopy in RME sections at day 5 and day 8 (Figure 2C). Whether gap junctions are involved in the barrier function has been investigated by treating RME with a previously determined non-cytotoxic concentration of 60 µM of carbenoxolone (CBX), a commonly used blocker of gap junctions. Our results showed that CBX had no direct impact on permeability to LY when RME at day 0 were treated for 6 hours (Figure 2B). Similarly, RME correctly stratified at day 5 and treated with CBX for 6 h retained their barrier property (not shown). However, when RME were treated with CBX for the last 72 h during their development to day 5, the barrier function was impaired, but this was mainly due to the altered differentiation/epidermal stratification, as evidenced by histological studies showing unstructured RME (data not shown). Together, these results confirmed that RME from day 3 to 8 formed a cohesive tissue and efficiently acquired their natural property of impermeable barrier.

### 3.3. RME response to proinflammatory cytokines

To complete the functional characterization of our RME model, we have investigated their response to cytokines relevant to skin inflammation. Firstly, we analyzed the basal expression of the different subunits of receptors for IL-22, OSM, IL-17A, TNF-α and IL-1α/β by RT-qPCR in RME at day 5 in comparison with normal epidermis. The expressions of TNFR1/R2, IL-10RB, gp130 and OSMRβ, IL-17RC, IL-1R1 and IL-1RAcP were similar between RME and normal epidermis, while IL-17RA and IL-22R1 exhibited a higher expression in the epidermis (Figure 3).

Then, RME at day 5 were stimulated either with IL-22, OSM, IL-17A, TNF-α or IL-1α at a final concentration of 10 ng/ml or a mix of these five cytokines (M5) at both concentrations of 10 ng/ml and 1 ng/ml. Histological analyses of RME were performed after 72 h of stimulation (Figure 4A). Stimulations with IL-1α, TNF-α or IL-22 did not change the morphological aspect of the epidermis. By contrast, IL-17A, OSM and M5 at the concentration of 1 ng/ml induced a modest hyperplasia with a significant reduction of keratohyalin granules in the granular layer, especially after OSM stimulation, while M5 stimulation at 10 ng/ml completely disrupted the stratified aspect of the RME. Regarding innate immunity markers, a strong synergistic induction of proinflammatory mediators including the antimicrobial peptides S100A9, BD3 and the chemokine CXCL3 was observed at the transcriptional level after RME stimulation with M5 at 10 ng/ml (Figure 4B). IL-1α, TNF-α and IL-22 also induced a modest expression of these proinflammatory markers, while IL-17A and OSM were found to be the most active on RME. These inductions of S100A9 were confirmed at the protein level by measuring S100A9 concentrations by ELISA in culture supernatants of RME 72 h after stimulation (Figure 4C). In correlation with the histological observations, the analysis of the mRNA expression of differentiation markers showed a strong downregulation of K10, filaggrin and involucrin 24 h after RME stimulation with OSM, IL-17A, M5 at 1 ng/ml and, to a lesser extent, with IL-1α, TNF-α and IL-22 (Figure 4D). M5 at the highest concentration strongly inhibited the expression of K10, loricrin and involucrin, 10-fold more than IL-17A or OSM alone, confirming the synergistic proinflammatory activity of the cytokine mix. A slight upregulation of K6 mRNA could also be observed in RME stimulated with OSM, IL-17A and M5 (Figure 4D), which was confirmed by confocal microscopy showing a positive immunostaining in the suprabasal layers of stimulated RME, including TNF-α-stimulated RME as well (Figure 4E). RME stimulated with OSM, IL-17A and M5 presented a specific and strong Cx26 immunostaining close to keratinocyte nuclei compared

to unstimulated RME, while the cornified layer harbored a non-specific staining (Figure 4E). No significant regulation of Cx43 expression by proinflammatory cytokines could be observed (data not shown). Finally, we performed permeability assays by measuring the concentrations of LY diffusing through RME 72 h after cytokine stimulation. In the non-treated condition, RME permeability to LY was very low (< 1% of maximal permeability) and the dye was retained in the cornified layer (Figures 4F and 4G). When RME were stimulated either with OSM or IL-17A alone, the barrier function was altered as assessed by the increased concentrations of LY in RME culture media reaching ~ 12% and 21% of maximal permeability, respectively (Figure 4F). As expected, in RME stimulated with M5 at the highest concentration, the structure of the epidermis was completely disrupted, allowing the massive diffusion of the dye through RME, as evidenced by the observation of LY staining under the cornified layer and the highest concentrations of LY in the lower chamber (~ 64% of maximal permeability; Figure 4F and 4G). Together these results confirm that RME are sensitive to proinflammatory cytokine stimulation and could be used to reproduce some the features of psoriatic skin, such as the production of inflammatory molecules and the altered epidermal differentiation.

## 4. Discussion

Few models of *in vitro* reconstituted epidermis from primary mouse keratinocytes are described, mainly due to the difficulty to maintain primary keratinocyte cultures and to reach a complete epidermal stratification, even by using established cultures of keratinocyte progenitors. Here, we propose a new protocol for the rapid and convenient generation of RME from primary NMEK, isolated from newborn mouse skin, harboring the structural and functional features of a normal epidermis. Cultures of primary keratinocytes isolated from adult skin presented limited proliferative capacity and our attempts to generate RME were not fully satisfactory. The best results were obtained when keratinocytes were isolated from 1 to 3 day-old mice. Indeed, primary mouse keratinocytes cultures from neonatal mice were shown to contain multiple progenitor cells, which are able to expand rapidly in few days (Kamimura, *et al.*, 1997). This method abrogates the use of murine keratinocyte progenitor cell lines, obtained after numerous passages as previously described (Segrelles, *et al.*, 2011, Vollmers, *et al.*, 2012), which need several weeks to reach a full epidermis-like structure. *In vitro* studies on mice skin equivalent models have also reported the dependence on the presence of a fibroblastic support or de-epidermised dermis for epidermis growth (Boehnke, *et al.*, 2007, Ikuta, *et al.*, 2006), thus complicating the protocol and introducing an additional inconstant parameter. In humans, the communication between fibroblasts and keratinocytes has been shown to be crucial for the formation of an efficient epidermis and a correct deposition of the basement membrane (El Ghalbzouri and Ponec, 2004). However, in human models, this fibroblastic dependence has been abrogated by introducing numerous and specific growth factors in keratinocyte culture media, including bovine pituitary extract, transferrin, hydrocortisone, L-ascorbic acid, $CaCl_2$ and KGF (Frankart, *et al.*, 2012). In our protocol, we have determined the optimal concentrations of these factors in the murine system to induce the differentiation and the complete stratification of keratinocytes without fibroblasts feeding.

We further characterized our model of RME by analyzing the expression of a panel of keratins and proteins involved in the formation of a stratified epidermis. Some studies suggested that *in vitro* murine epidermis equivalents were thicker than a normal murine epidermis (Ikuta, *et al.*, 2006). Our protocol generates RME at day 5 with a thickness comparable to a normal mouse epidermis (~ 20-25 µm) with only two or three layers of stacked keratinocytes. The expression of K14 was normally restricted to the basal layer, as in normal mouse skin. As well, K6 expression was also found close the basement membrane, with a high expression at days 3 and 5, but decreasing progressively from day 8 along with the thickening of the cornified layer which precedes RME degeneration. This high expression of K6 is a common feature of reconstituted epidermis models and it has been proposed that the protocols mimic an *in vivo* wound healing process in which K6 is overexpressed (Rosenberger, *et al.*, 2014, Segrelles, *et al.*, 2011, Stark, *et al.*, 1999). Furthermore, labeling of K10, filaggrin and loricrin revealed their appropriate localization in the suprabasal and granular layers of RME. As RME from day 8 change their morphology and their K6 expression profile, we propose to use RME at day 5 for functional studies. For further characterization, we also analyzed the expression of connexins, which play an important role in the coordination of keratinocyte proliferation/differentiation balance during epidermis morphogenesis. A previous report described Cx43 localization in proliferating keratinocytes and a Cx26 labeling in the granular layer (Kandyba, *et al.*, 2008). We found the same localization in our model but Cx26 expression level seemed to be more elevated in RME than in normal epidermis. Similarly to K6 expression, Cx26 has been reported to be upregulated in a context of wound healing (Churko and Laird, 2013, Kretz, *et al.*, 2003), suggesting the activated state of isolated primary keratinocytes engaged in a process of epidermis reconstitution. Treatments of RME with the gap junction blocker CBX suggested that connexins contribute indirectly to the barrier function of RME and are mostly involved in

epidermal differentiation and the complete stratification of RME. Finally, the cohesive structure of RME was demonstrated by the homogenous expression of E-cadherin throughout the structured epidermis and the constitution of a functional impermeable epidermal barrier.

As most of studies on mouse epidermis were carried out *in vivo*, how differentiated murine keratinocytes respond individually to cytokine stimulation *in vitro* is poorly documented. Thus, to complete the functional characterization of our RME, we analyzed their response to proinflammatory cytokines previously described to target keratinocytes and to be involved in psoriasis (Guilloteau, *et al.*, 2010). After showing that RME expressed all the subunits of cytokine receptors studied in this work, we evaluated their individual and synergistic activities, allowing a parallel with the human system. The mix of five cytokine, M5, induced a complete disruption of the structure of the RME and a downregulation of the expression of genes involved in epidermal differentiation. M5 stimulation reproduced also some features of inflammatory keratinocytes through the secretion of antimicrobial peptides and chemokines. These results were comparable to those observed in cytokine-stimulated RHE previously described (Guilloteau et al., 2010), highlighting similarities between human and mouse systems. Nonetheless, some differences could be observed between the two species. In RME stimulated by single cytokines, only IL-17A and OSM could disrupt the cornified layer by inhibiting epidermal differentiation. These cytokines were also shown to be the most active to induce a proinflammatory phenotype in murine keratinocytes (Guilloteau, *et al.*, 2010, Pohin, *et al.*, 2016). Interestingly, IL-17 and OSM are the two cytokines that provoke a strong induction of Cx26 expression and an alteration of the barrier property of RME. This upregulation of Cx26 has been described in inflammatory conditions such as psoriatic skin (Labarthe, *et al.*, 1998) , wound healing (Churko and Laird, 2013, Kretz, *et al.*, 2003), in a model of RHE under stress conditions (Wiszniewski, *et al.*, 2000) and was shown to be associated with profound barrier impairment in a model of transgenic mice overexpressing

Cx26 in the skin (Djalilian, *et al.*, 2006). By contrast, in humans, IL-22 and OSM were shown to be the most potent inhibitors of epidermal differentiation, in particular by inducing STAT-3 activation pathway (Rabeony, *et al.*, 2014), whereas IL-1, IL-17A and TNF-α were mainly involved in the induction of innate immunity mediators (Guilloteau, *et al.*, 2010). In our hands, IL-22 was not as active as OSM on RME. This might be explained by the lowered expression of the IL-22R1 chain in our RME compared to its expression in normal epidermis. Finally, IL-1α and TNF-α were also active on keratinocytes but failed to induce structural changes in RME formation. The regulation of the inflammatory markers induced by these two cytokines alone is limited but in a complex network involving multiple cytokines, such as in atopic dermatitis or psoriasis, it is likely that they contribute to cytokine synergy increasing disease severity.

In conclusion, we propose a new protocol for the formation of a complete RME in five days which tends to reproduce closely the tissue architecture of a normal epidermis. These RME have an intact barrier function and are able to respond to cytokines relevant to skin inflammation, similarly to what has been described in the human system. This new model of RME would greatly contribute to study the normal differentiation of epidermis or its alteration in inflammatory conditions. Moreover, this model opens the possibility to generate RME from genetically engineered mice to further dissect the role of the transgene (knock-in or knock-down) on the physiology of the epidermis.

## Conflict of Interest

The authors have declared that there is no conflict of interest.

## Acknowledgements

We thank Dr. Anne Cantereau (ImageUP, Université de Poitiers) for technical assistance in confocal microscopy, Dr. Michel Simon (INSERM U1056, Université de Toulouse) for the protocol of Lucifer Yellow assay and Pr. Guylène Page (Université de Poitiers) for the use of the Varioskan. This study was supported by grants from a clinical research program from Poitiers University Hospital, « la Ligue contre le Cancer », « le Cancéropôle Grand Ouest », « l'Association Nationale de Recherche et de la Technologie », ECOS-Sud committee and from "Le conseil régional de la région Poitou-Charentes". M. P. is supported by "Le conseil régional de la région Poitou-Charentes".

## Author Contributions

MP, CB, JG, JFJ designed protocols for RME generation. MP, CV, JG, CB, JFJ performed the experiments. MP, CV, JG, CB, LC, VH, LF, JM, FXB, FM, JCL, JFJ analyzed and interpreted the data. MP, JFJ wrote the manuscript. JFJ designed the research. All the authors read and approved the final manuscript.

## Figure legends

**Figure 1. RME reproduce the structure and the expression profiles of differentiation markers of a normal mouse epidermis.**

(A) Schematic representation of the main steps for RME formation. (B) H&E histology of RME at days 3, 5 and 8 and normal mouse skin sections (upper panel). Scale bar, 20 µm. Immunofluorescent staining for K6, K14 and K10, loricrin and filaggrin (all in red) and TOPRO-3 staining for cell nuclei (in blue). Original magnification: ×600. The dotted white line delineates the dermal-epidermal junction of mouse skin or the membrane of the insert for RME. The solid white line marks the surface of the epidermis of mouse skin and RME. Images are representative of three independent experiments.

**Figure 2. RME express GAP and adherence junctions and acquire their natural barrier function.**

(A) Immunofluorescent staining of RME at days 3, 5 and 8 and normal mouse skin sections were performed with primary antibodies specific for E-cadherin (in red), Cx43 and Cx26 (both in green) and TOPRO-3 staining for cell nuclei (in blue). For details, see insets. The dotted white line delineates the dermal-epidermal junction of mouse skin or the membrane of the insert for RME. The solid white line marks the surface of the epidermis of mouse skin and RME. Images are representative of three independent experiments. Original magnification: ×600. (B) Quantification of RME permeability to Lucifer Yellow (LY). Concentrations of LY passing through RME were measured in culture media, 6 h after dye deposition on the surface of RME at days 0, 3, 5 and 8 (n=3), or RME at day 0 in the presence of 60 µM of carbenoxolone (CBX). Data are expressed as mean ± SEM percentage of the maximal

permeability for LY, previously determined by measuring LY concentrations that diffused through the polycarbonate membrane insert without keratinocytes. Data are from three independent experiments. (C) Lucifer Yellow staining (in green) by confocal microscopy, 6 h after dye deposition on the surface of RME at day 5 and day 8. Cell nuclei were stained with TOPRO-3 (in blue).The dotted white delineates the membrane of the insert. Original magnification: ×600.

**Figure 3. RME express cytokine receptors similarly to a normal epidermis.**

Transcriptional analysis by RT-qPCR was performed for the indicated subunits of cytokine receptors in RME at 5 day and in normal epidermis. Data represent mean ± SEM expression level of the gene of interest relative to the expression of the housekeeping gene GAPDH, from 4 independent experiments. *$p < 0.05$; using two-way ANOVA followed by Bonferroni post-test.

**Figure 4. RME respond to skin-relevant proinflammatory cytokines by an altered differentiation and barrier function.**

RME at day 5 were stimulated with the indicated single cytokines at the concentration of 10 ng/ml and the mix of 5 cytokines, M5, at 1 and 10 ng/ml, respectively. (A) After 72 h of stimulation, RME histology was examined after H&E staining. NS, non-stimulated. Scale bar, 20 µm. (B) After 24 h of stimulation, the expression of genes involved in the innate immune response of keratinocytes including S100A9, CXCL-3 and BD3 was determined by RT-qPCR. Data represent mean ± SEM mRNA fold change above unstimulated RME, from 4 independent experiments. (C) Mean ± SEM S100A9 concentrations measured by ELISA in

culture media of RME 72 h after cytokine stimulation. Data are from three independent experiments. (D) After 24 h of stimulation, the expression of the epidermal differentiation genes K6, K10, filaggrin and involucrin was determined by RT-qPCR. Data represent mean ± SEM mRNA fold change above unstimulated RME, from 4 independent experiments. (E) Immunofluorescent staining of cytokine-stimulated RME was performed with primary antibodies specific for Cx26 (in green) and K6 (in red). (F) Quantification of RME permeability to LY after cytokine stimulation for 72 h. Data are expressed as mean ± SEM percentage of the maximal permeability for LY, from three independent experiments. (G) Fluorescence detection by confocal microscopy of LY (in green) in sections of non-stimulated (NS) and M5-stimulated RME, 6 h after dye deposition. Cell nuclei were stained with TOPRO-3 (in blue) and the dotted white delineates the membrane of the insert. Original magnification: ×600.

## References


Bertolero F, Kaighn ME, Gonda MA, *et al.* 1984, Mouse epidermal keratinocytes. Clonal proliferation and response to hormones and growth factors in serum-free medium, *Exp Cell Res*, **155** (1): 64-80.

Boehnke K, Mirancea N, Pavesio A, *et al.* 2007, Effects of fibroblasts and microenvironment on epidermal regeneration and tissue function in long-term skin equivalents, *Eur J Cell Biol*, **86** (11-12): 731-746.

Boniface K, Bernard FX, Garcia M, *et al.* 2005, IL-22 inhibits epidermal differentiation and induces proinflammatory gene expression and migration of human keratinocytes, *J Immunol*, **174** (6): 3695-3702.

Boniface K, Diveu C, Morel F, *et al.* 2007, Oncostatin M secreted by skin infiltrating T lymphocytes is a potent keratinocyte activator involved in skin inflammation, *J Immunol*, **178** (7): 4615-4622.

Borowiec AS, Delcourt P, Dewailly E, *et al.* 2013, Optimal differentiation of in vitro keratinocytes requires multifactorial external control, *PLoS One*, **8** (10): e77507.

Candi E, Schmidt R, Melino G. 2005, The cornified envelope: a model of cell death in the skin, *Nat Rev Mol Cell Biol*, **6** (4): 328-340.

Carroll JM, Moles JP. 2000, A three-dimensional skin culture model for mouse keratinocytes: application to transgenic mouse keratinocytes, *Exp Dermatol*, **9** (1): 20-24.

Churko JM, Laird DW. 2013, Gap junction remodeling in skin repair following wounding and disease, *Physiology (Bethesda)*, **28** (3): 190-198.

Djalilian AR, McGaughey D, Patel S, *et al.* 2006, Connexin 26 regulates epidermal barrier and wound remodeling and promotes psoriasiform response, *J Clin Invest*, **116** (5): 1243-1253.

El Ghalbzouri A, Ponec M. 2004, Diffusible factors released by fibroblasts support epidermal morphogenesis and deposition of basement membrane components, *Wound Repair Regen*, **12** (3): 359-367.

Frankart A, Malaisse J, De Vuyst E, *et al.* 2012, Epidermal morphogenesis during progressive in vitro 3D reconstruction at the air-liquid interface, *Exp Dermatol*, **21** (11): 871-875.

Guenou H, Nissan X, Larcher F, *et al.* 2009, Human embryonic stem-cell derivatives for full reconstruction of the pluristratified epidermis: a preclinical study, *Lancet*, **374** (9703): 1745-1753.

Guilloteau K, Paris I, Pedretti N, *et al.* 2010, Skin Inflammation Induced by the Synergistic Action of IL-17A, IL-22, Oncostatin M, IL-1alpha, and TNF-alpha Recapitulates Some Features of Psoriasis, *J Immunol*, **184** (9): 5263-5270.

Hennings H, Michael D, Cheng C, *et al.* 1980, Calcium regulation of growth and differentiation of mouse epidermal cells in culture, *Cell*, **19** (1): 245-254.

Ikuta S, Sekino N, Hara T, *et al.* 2006, Mouse epidermal keratinocytes in three-dimensional organotypic coculture with dermal fibroblasts form a stratified sheet resembling skin, *Biosci Biotechnol Biochem*, **70** (11): 2669-2675.

Kamimura J, Lee D, Baden HP, *et al.* 1997, Primary mouse keratinocyte cultures contain hair follicle progenitor cells with multiple differentiation potential, *J Invest Dermatol*, **109** (4): 534-540.

Kandyba EE, Hodgins MB, Martin PE. 2008, A murine living skin equivalent amenable to live-cell imaging: analysis of the roles of connexins in the epidermis, *J Invest Dermatol*, **128** (4): 1039-1049.

Kretz M, Euwens C, Hombach S, *et al.* 2003, Altered connexin expression and wound healing in the epidermis of connexin-deficient mice, *J Cell Sci*, **116** (Pt 16): 3443-3452.

Labarthe MP, Bosco D, Saurat JH, *et al.* 1998, Upregulation of connexin 26 between keratinocytes of psoriatic lesions, *J Invest Dermatol*, **111** (1): 72-76.

Moll R, Divo M, Langbein L. 2008, The human keratins: biology and pathology, *Histochem Cell Biol*, **129** (6): 705-733.

Pendaries V, Malaisse J, Pellerin L, *et al.* 2014, Knockdown of filaggrin in a three-dimensional reconstructed human epidermis impairs keratinocyte differentiation, *J Invest Dermatol*, **134** (12): 2938-2946.

Pohin M, Guesdon W, Mekouo AA, *et al.* 2016, Oncostatin M overexpression induces skin inflammation but is not required in the mouse model of imiquimod-induced psoriasis-like inflammation, *Eur J Immunol*, **46** (7): 1737-1751.

Ponec M, Weerheim A, Kempenaar J, *et al.* 1997, The formation of competent barrier lipids in reconstructed human epidermis requires the presence of vitamin C, *J Invest Dermatol*, **109** (3): 348-355.

Poumay Y, Coquette A. 2007, Modelling the human epidermis in vitro: tools for basic and applied research, *Arch Dermatol Res*, **298** (8): 361-369.

Prunieras M, Regnier M, Woodley D. 1983, Methods for cultivation of keratinocytes with an air-liquid interface, *J Invest Dermatol*, **81** (1 Suppl): 28s-33s.

Rabeony H, Petit-Paris I, Garnier J, *et al.* 2014, Inhibition of keratinocyte differentiation by the synergistic effect of IL-17A, IL-22, IL-1alpha, TNFalpha and oncostatin M, *PLoS One*, **9** (7): e101937.

Rabeony H, Pohin M, Vasseur P, *et al.* 2015, IMQ-induced skin inflammation in mice is dependent on IL-1R1 and MyD88 signaling but independent of the NLRP3 inflammasome, *Eur J Immunol*, **45** (10): 2847-2857.

Rheinwald JG, Green H. 1975, Formation of a keratinizing epithelium in culture by a cloned cell line derived from a teratoma, *Cell*, **6** (3): 317-330.

Rosdy M, Clauss LC. 1990, Terminal epidermal differentiation of human keratinocytes grown in chemically defined medium on inert filter substrates at the air-liquid interface, *J Invest Dermatol*, **95** (4): 409-414.

Rosenberger S, Dick A, Latzko S, *et al.* 2014, A mouse organotypic tissue culture model for autosomal recessive congenital ichthyosis, *Br J Dermatol*, **171** (6): 1347-1357.

Scott CA, Tattersall D, O'Toole EA, *et al.* 2012, Connexins in epidermal homeostasis and skin disease, *Biochim Biophys Acta*, **1818** (8): 1952-1961.

Segrelles C, Holguin A, Hernandez P, *et al.* 2011, Establishment of a murine epidermal cell line suitable for in vitro and in vivo skin modelling, *BMC Dermatol*, **11**: 9.

Simpson CL, Patel DM, Green KJ. 2011, Deconstructing the skin: cytoarchitectural determinants of epidermal morphogenesis, *Nat Rev Mol Cell Biol*, **12** (9): 565-580.

Stark HJ, Baur M, Breitkreutz D, *et al.* 1999, Organotypic keratinocyte cocultures in defined medium with regular epidermal morphogenesis and differentiation, *J Invest Dermatol*, **112** (5): 681-691.

Tu CL, Bikle DD. 2013, Role of the calcium-sensing receptor in calcium regulation of epidermal differentiation and function, *Best Pract Res Clin Endocrinol Metab*, **27** (3): 415-427.

Tu CL, Chang W, Xie Z, *et al.* 2008, Inactivation of the calcium sensing receptor inhibits E-cadherin-mediated cell-cell adhesion and calcium-induced differentiation in human epidermal keratinocytes, *J Biol Chem*, **283** (6): 3519-3528.

Vollmers A, Wallace L, Fullard N, *et al.* 2012, Two- and three-dimensional culture of keratinocyte stem and precursor cells derived from primary murine epidermal cultures, *Stem Cell Rev*, **8** (2): 402-413.

Wilson NJ, Boniface K, Chan JR, *et al.* 2007, Development, cytokine profile and function of human interleukin 17-producing helper T cells, *Nat Immunol*, **8** (9): 950-957.

Wiszniewski L, Limat A, Saurat JH, *et al.* 2000, Differential expression of connexins during stratification of human keratinocytes, *J Invest Dermatol*, **115** (2): 278-285.

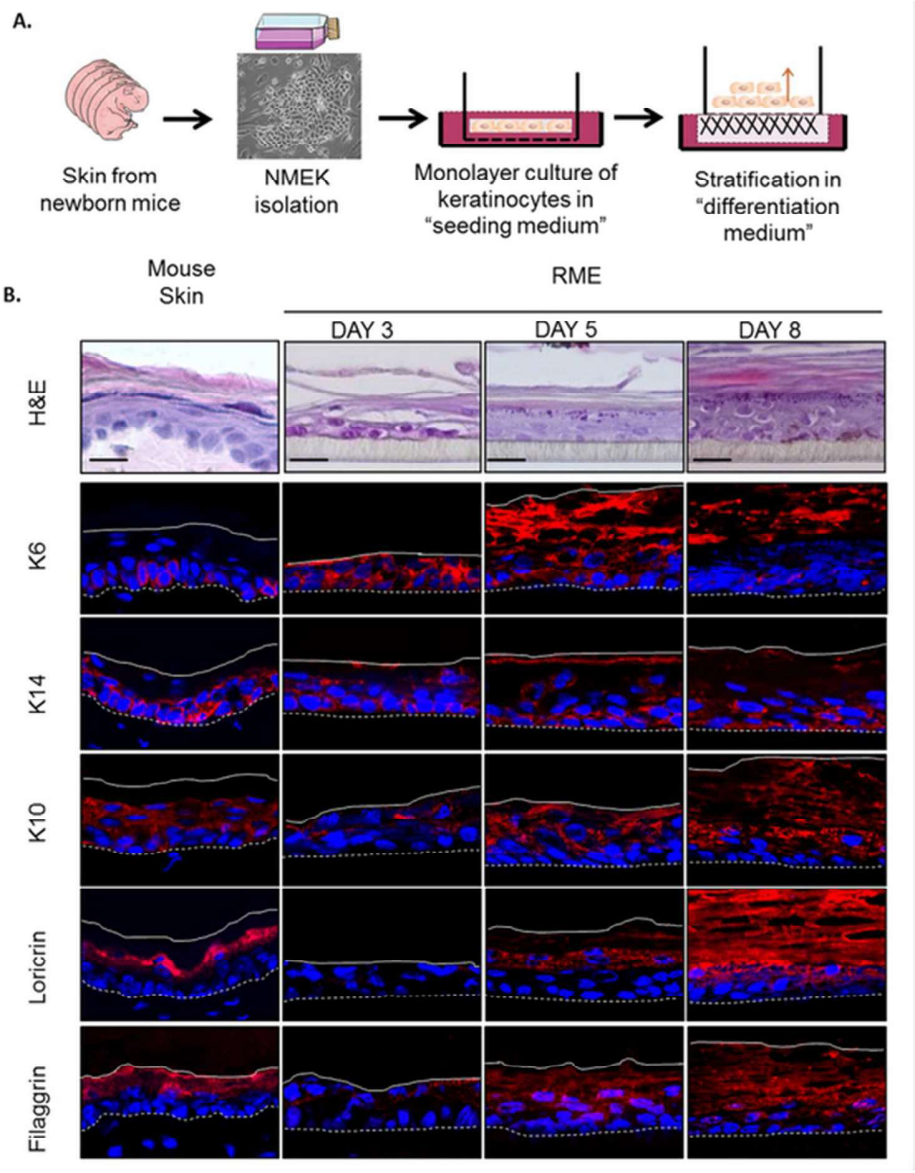


Figure 1

50x64mm (300 x 300 DPI)

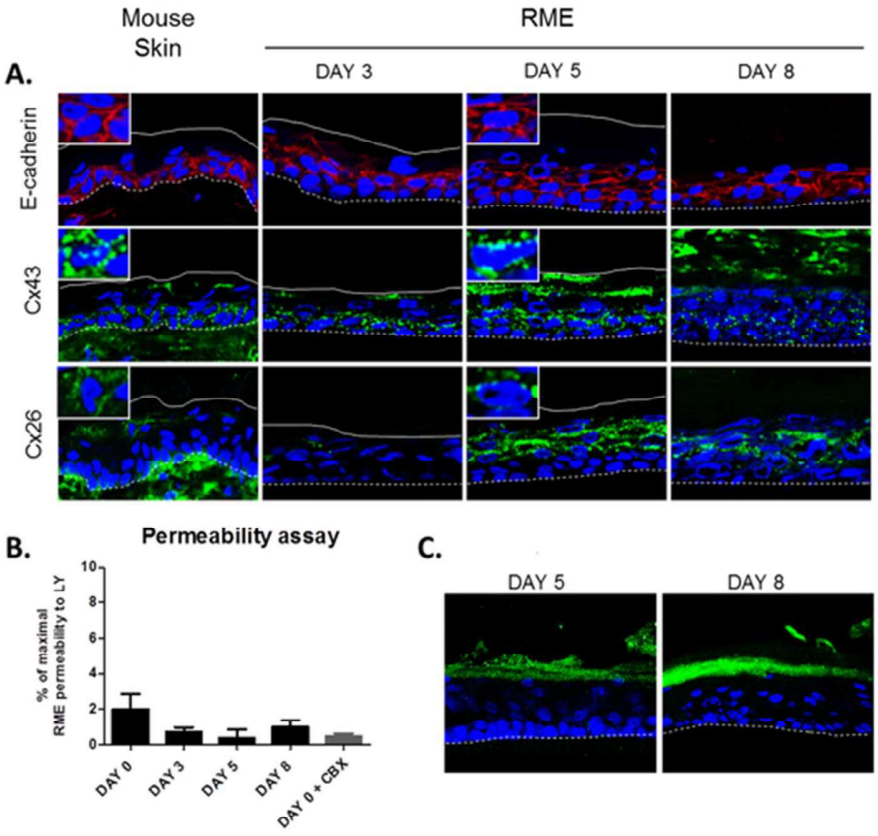


Figure 2

50x45mm (300 x 300 DPI)

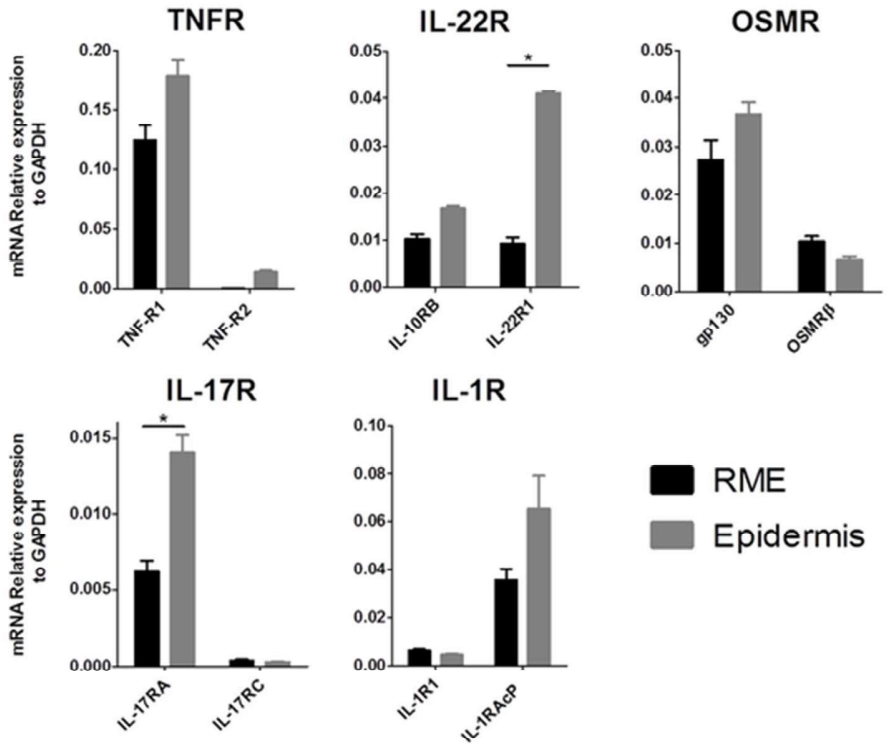


Figure 3

50x42mm (300 x 300 DPI)

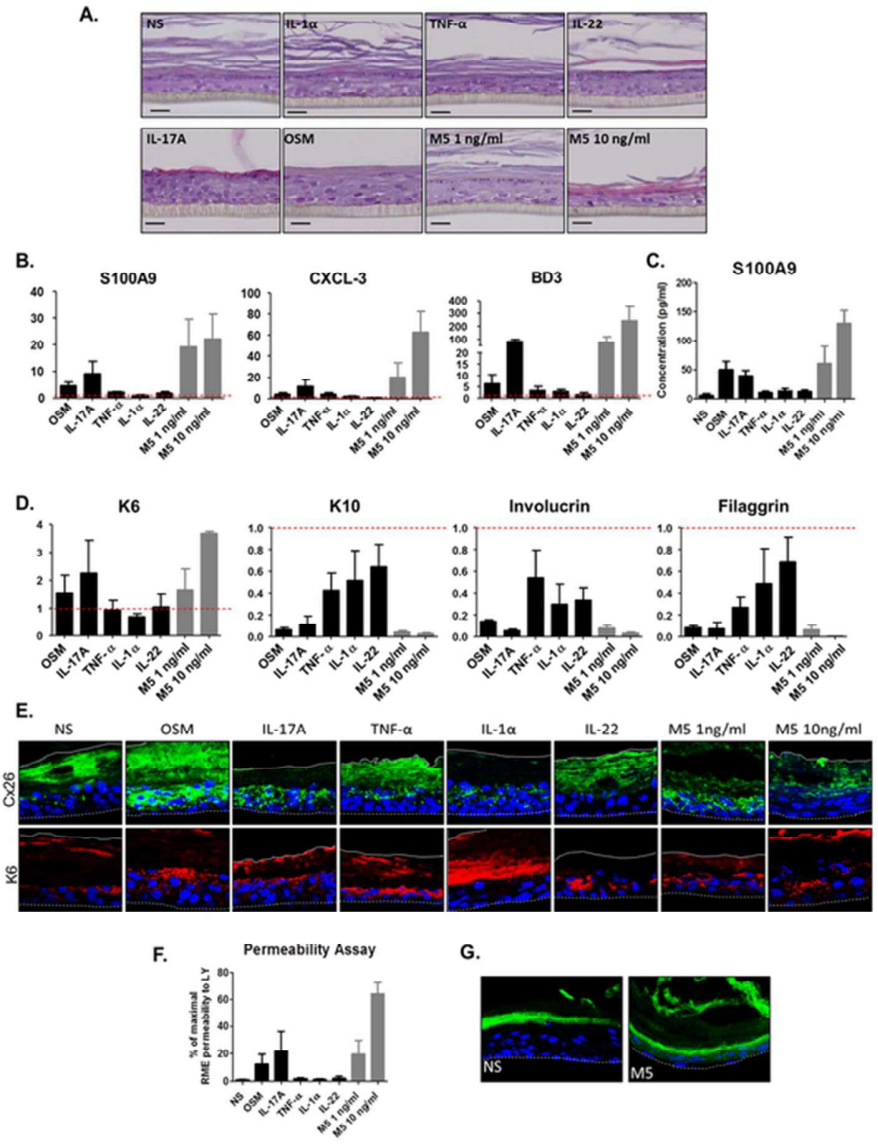


Figure 4

50x67mm (300 x 300 DPI)